The Journal of Immunology

Evasion of Innate Cytosolic DNA Sensing by a Gammaherpesvirus Facilitates Establishment of Latent Infection

Chenglong Sun, Stefan A. Schattgen, Prapaporn Pisitkun, Joan P. Jorgensen, Adam T. Hilterbrand, Lucas J. Wang, John A. West, Kathrine Hansen, Kristy A. Horan, Martin R. Jakobsen, Peter O'Hare, Heiko Adler, Ren Sun, Hidde L. Ploegh, Blossom Damania, Jason W. Upton, Katherine A. Fitzgerald and Søren R. Paludan

J Immunol published online 16 January 2015
http://www.jimmunol.org/content/early/2015/01/16/jimmunol.1402495

The Journal of Immunology is published twice each month by The American Association of Immunologists, Inc., 9650 Rockville Pike, Bethesda, MD 20814-3994.

Print ISSN: 0022-1767 Online ISSN: 1550-6606.

Published January 16, 2015, doi:10.4049/jimmunol.1402495

Evasion of Innate Cytosolic DNA Sensing by a Gammaherpesvirus Facilitates Establishment of Latent Infection

Chenglong Sun,*,†,1 Stefan A. Schattgen,‡,1 Prapaporn Pisitkun,*,†,§,1 Joan P. Jorgensen,*,†,1 Adam T. Hilterbrand,¶ Lucas J. Wang,¶ John A. West,‖ Kathrine Hansen,*,† Kristy A. Horan,* Martin R. Jakobsen,*,† Peter O'Hare,# Heiko Adler, Ren Sun,†† Hidde L. Ploegh,‡‡ Blossom Damania,‖ Jason W. Upton,¶ Katherine A. Fitzgerald,‡ and Søren R. Paludan*,†**

Herpesviruses are DNA viruses harboring the capacity to establish lifelong latent-recurrent infections. There is limited knowledge about viruses targeting the innate DNA-sensing pathway, as well as how the innate system impacts on the latent reservoir of herpesvirus infections. In this article, we report that murine gammaherpesvirus 68 (MHV68), in contrast to α- and β-herpesviruses, induces very limited innate immune responses through DNA-stimulated pathways, which correspondingly played only a minor role in the control of MHV68 infections in vivo. Similarly, Kaposi's sarcoma–associated herpesvirus also did not stimulate immune signaling through the DNA-sensing pathways. Interestingly, an MHV68 mutant lacking deubiquitinase (DUB) activity, embedded within the large tegument protein open reading frame (ORF)64, gained the capacity to stimulate the DNA-activated stimulator of IFN genes (STING) pathway. We found that ORF64 targeted a step in the DNA-activated pathways upstream of the bifurcation into the STING and absent in melanoma 2 pathways, and lack of the ORF64 DUB was associated with impaired delivery of viral DNA to the nucleus, which, instead, localized to the cytoplasm. Correspondingly, the ORF64 DUB active site mutant virus exhibited impaired ability to establish latent infection in wild-type, but not STING-deficient, mice. Thus, gammaherpesviruses evade immune activation by the cytosolic DNA-sensing pathway, which, in the MHV68 model, facilitates establishment of infections. ***The Journal of Immunology*****, 2015, 194: 000–000.**

Herpesviruses are capable of establishing latent-recurrent infections, and can give rise to disease in both the acute and recurrent phase, mainly in immunosuppressed individuals. Herpesviruses are DNA viruses that enter cells through the plasma membrane or an endosomal route and shuttle through the cytoplasm for delivery of DNA to the nucleus where productive replication takes place (1). Three subclasses of herpesviruses exist, termed α-, β-, and γ-herpesviruses, which have a common set of properties, as well as functions specific for the different subfamilies. Advances in the field of innate immunology revealed important roles for the innate immune system in host control of herpesvirus infections (2–4). In corroboration with this notion, knowledge on herpesviruses evading innate immune responses is now starting to emerge (5), but information on how this impacts on the establishment of acute and latent infections is still lacking. Therefore, in this study we hypothesized that herpesviruses target key elements of the innate immune system with the purpose of facilitating the establishment of latent infection.

Nucleic acids are believed to be the main inducers of innate immunity during viral infection (6), with type I IFN production and inflammasome-dependent IL-1β maturation being two important biological responses evoked by these viral molecules.

*Department of Biomedicine, Aarhus University, DK-8000 Aarhus C, Denmark; †Aarhus Research Center for Innate Immunology, Aarhus University, DK-8000 Aarhus C, Denmark; ‡Division of Infectious Diseases and Immunology, Department of Medicine, University of Massachusetts Medical School, Worcester, MA 01655; §Department of Medicine, Ramathibodi Hospital, Mahidol University, Bangkok, Thailand 10400; ¶Department of Molecular Biosciences, Institute for Cellular and Molecular Biology, University of Texas at Austin, Austin, TX 78712; ‖Department of Microbiology and Immunology, University of North Carolina, Chapel Hill, Chapel Hill, NC 27599; #Section of Virology, Faculty of Medicine, Imperial College, St. Mary's Campus, London W2 1PG, United Kingdom; **Helmholtz Zentrum Munich, German Research Center for Environmental Health, D-81377 Munich, Germany; ††Department of Molecular Biology and Medical Pharmacology, Faculty of Medicine, University of California, Los Angeles, Los Angeles, CA 90095; and ‡‡Whitehead Institute for Biomedical Research, Cambridge, MA 02142

[1]C.S., S.A.S., P.P., and J.P.J. contributed equally to this work.

Received for publication October 2, 2014. Accepted for publication December 13, 2014.

This work was supported by Danish Medical Research Council Grants 09-072636 and 12-124330, the Novo Nordisk Foundation, the Velux Foundation, Lundbeck Foundation Grant R34-3855, the Kathrine og Vigo Skovgaardes Fond, the Elvira og Rasmus Riisforts Almenvelgørende Fond, and the Fonden til Lægevidenskabens Fremme (all to S.R.P.). This work also was supported by National Institutes of Health Grants AI083713 and AI093752 (to K.A.F.) and AI109965, AI107810, CA019014, and DE018281 (to B.D.), as well as Cancer Prevention and Research Institute of Texas Grant R1202 (to J.W.U.). C.S. was funded by China Scholarship Council Scholarship 201206170055, and K.A.H. was funded by a Marie Curie Incoming International Fellowship.

Address correspondence and reprint requests to Dr. Søren R. Paludan, Department of Biomedicine, Aarhus University, Wilhelm Meyers Allé 4, DK-8000 Aarhus C, Denmark. E-mail address: srp@biomed.au.dk

The online version of this article contains supplemental material.

Abbreviations used in this article: AIM2, absent in melanoma 2; BAC, bacterial artificial chromosome; BMDC, bone marrow–derived DC; BMM, bone marrow–derived macrophage; cGAMP, cyclic GMP-AMP; cGAS, cGAMP synthetase; DC, dendritic cell; DUB, deubiquitinase; EdC, deoxy-5-ethynylcytidine; IFI, IFN inducible protein; KSHV, Kaposi's sarcoma–associated herpesvirus; MCMV, murine CMV; MHV68, murine gammaherpesvirus 68; MOI, multiplicity of infection; ORF, open reading frame; poly(dA:dT), poly(deoxyadenylic-deoxythymidylic) acid; poly I:C, polyinosinic-polycytidylic acid; shRNA, short hairpin RNA; STING, stimulator of IFN genes; TBK1, Tank-binding kinase-1; WT, wild-type.

For herpesviruses, it is known that viral RNA and DNA are detected by endosomal TLRs, as well as cytoplasmic RNA sensors (3, 7–9). Recently, much focus has been on intracellular DNA, and it is now emerging that viral DNA in the cytoplasm and the nucleus can also trigger the innate immune system (4, 10–15). In vivo studies revealed important roles for DNA-sensing pathways in host protection against herpesvirus infections (2, 4). Common to the IFN-stimulating pathways triggered by intracellular DNA is the requirement for stimulator of IFN genes (STING) (2). STING is a tetra-membrane spanning endoplasmic reticulum protein that translocates to specific vesicular structures after DNA recognition, where signaling is believed to take place (2). Cytosolic DNA also stimulates inflammasome activation through a pathway dependent on absent in melanoma 2 (AIM2) and, in this manner, leads to assembly of a caspase 1–containing complex capable of cleaving pro–IL-1β and pro–IL-18 into the biologically active forms (16).

We recently demonstrated that genomic DNA of α-herpesviruses (HSV) and β-herpesviruses (CMV) is detected by DNA sensors in the cytosol after degradation of the capsid (17). Detection of HSV and CMV DNA was reported to involve the DNA sensors IFN inducible protein (IFI)16 and cyclic GMP-AMP (cGAMP) synthetase (cGAS), with the latter stimulating cGAMP-mediated STING-dependent signaling and induction of type I IFN expression (15, 17). It is also documented that CMV stimulates inflammasome activation in a manner that is dependent on AIM2 (4). The subfamily of gammaherpesviruses includes the human pathogenic viruses EBV and Kaposi's sarcoma–associated herpesvirus (KSHV) and the murine gammaherpesvirus 68 (MHV68). All of these viruses are detected by TLR9 in plasmacytoid dendritic cells (DCs) (9, 18, 19), and it was reported that IFI16 detects KSHV DNA in the nucleus of endothelial cells to induce caspase 1 activation and pro–IL-1β maturation (14). However, despite the importance of STING and AIM2 in the response to α- and β-herpesvirus infections, there is limited information on the role of the DNA-activated pathways in innate responses to gammaherpesvirus infections. Moreover, information on the impact of innate immune activation on the establishment of the latent reservoir of herpesvirus infections is still sparse.

In this article, we report that the gammaherpesviruses MHV68 and KSHV, in contrast to α- and β-herpesviruses, only weakly induce innate immune responses through DNA-stimulated pathways. We identified that an open reading frame (ORF)64 deubiquitinase (DUB)-deficient MHV68 mutant gained the capacity to induce type I IFN through the DNA-activated STING pathway, suggesting an essential role for DUB in evading host immune activation. Importantly, the MHV68 ORF64 mutant virus exhibited an impaired ability to establish latent infection in wild-type (WT), but not in STING-deficient, mice. Collectively, these data suggest that gammaherpesviruses evade immune activation by the cytosolic DNA–sensing pathway via the DUB activity embedded in the viral tegument and that this contributes to the ability of these viruses to establish latent infections.

Materials and Methods

Mice

For this study, we used C57BL/6, TLR3$^{-/-}$, TLR2/9$^{-/-}$, STING$^{gt/gt}$, ASC$^{-/-}$, NLRP3$^{-/-}$, and AIM2$^{-/-}$ mice. C57BL/6, TLR3$^{-/-}$, TLR2/9$^{-/-}$, and STING$^{gt/gt}$ mice were kept in the animal facility of the Faculty of Health, Aarhus University, whereas ASC$^{-/-}$, NLRP3$^{-/-}$, and AIM2$^{-/-}$ mice were kept in the animal facility of the University of Massachusetts Medical School. All mice were housed in a specific pathogen–free environment.

Viruses

MHV68 used in this study was the WUMS strain. MHV68 was propagated and titrated in BHK-21 hamster kidney cells in Glasgow modified essential medium. For select experiments, we used bacterial artificial chromosome (BAC)-derived MHV68-GFP (20). The ORF64 C33A mutant and the ORF36 N36S mutant, as well as the corresponding revertant viruses, were produced as previously described (21, 22). KSHV was produced as described previously (9). Briefly, baculovirus ORF50 was amplified in Sf9 cells. Vero cells stably expressing KSHV-GFP were infected with baculovirus ORF50 and treated with 2 mM sodium butyrate to allow reactivation of the latent KSHV. At 72 h, supernatant was harvested and passed through a sterile 0.45-μM filter. Virus concentration was performed by layering virus supernatant over a cushion of 20% sucrose. The virus was pelleted by ultracentrifugation for 2 h at 4˚C at 24,000 rpm, and the pellets were resuspended in endotoxin-free sterile Dulbecco's PBS.

HSV-1 (KOS strain) and the VP1-2 C65A mutant (23) were amplified in Vero cells. Murine CMV (MCMV) mutagenesis, diagnosis, and propagation were performed essentially as previously described (24). MCMV-K181 BAC [accession AM886412.1 (25)] was used to generate MCMV-M48 (C23S) by recombineering using a two-step allelic exchange. Briefly, a selection/counter-selection cassette was used to replace nt 67,098–67,111 of the WT MCMV BAC, which, in turn, was replaced with a PCR amplicon containing synonymous substitutions to introduce a unique diagnostic restriction site and a T-to-A substitution mutation at genomic position 67109, changing codon 23 of M48 from cysteine (TGC) to serine (AGC). Recombinant BACs were selected and confirmed by PCR and restriction fragment length polymorphism analysis. Infectious virus was reconstituted as previously described (24), amplified by growth in STO cells (ATCC CRL-1503) in the presence of 25 μg/ml 6-thioguanine (Sigma-Aldrich, St. Louis, MO), and plaque purified by limiting dilution. Then, parental and mutant viral stocks were generated as previously described (24) in NIH3T3 fibroblasts or IFNAR1$^{-/-}$ mouse embryonic fibroblasts. Virus preparations were tested for endotoxin content, and all were found to contain similar low levels (~0.75 endotoxin units/ml).

Reagents

For in vitro–stimulation experiments, we used dsDNA (HSV60mer, 2 μg/ml), cGAMP (2 μM), polyinosinic-polycytidylic acid (poly I:C; 25 μg/ml), ODN1826 (5 μM), Pam3CSK4 (200 ng/ml; all from InvivoGen), LPS (200 ng/ml), poly(deoxyadenylic-deoxythymidylic) acid [poly(dA:dT)] (1 μg/ml; Sigma-Aldrich), nigericin (10 μM; Sigma-Aldrich), and recombinant murine IFN-β and TNF-α (both from R&D Systems). The HSV-1 60mer is derived from the HSV-1 genome nt 144,107–144,166 and was obtained from DNA Technology (26). For transfection, the DNA was complexed with Lipofectamine 2000 (Invitrogen, Carlsbad, CA) and transfected into the cells, according to the manufacturer's instructions.

Primary murine bone marrow–derived cells

Bone marrow cells were harvested from the hind legs of mice. Cells were cultured in growth media (RPMI 1640 medium with 10% heat-inactivated FCS, 600 μg/ml glutamine, 200 IU/ml penicillin, and 100 μg/ml streptomycin [Life Technologies]) and stimulated with a concentration of 40 ng/ml GM-CSF (R&D Systems). On days 3 and 5, fresh GM-CSF was added. On day 7, the nonadherent bone marrow–derived DCs (BMDCs) and the adherent bone marrow–derived macrophages (BMMs) were harvested. For experiments, cells were seeded in RPMI 1640 medium with 10% FCS at a density of 200,000 cells/cm^2.

Human monocyte/macrophage cell line

THP1 cells (American Type Culture Collection) were cultured as nonadherent monocyte-like cells in growth media (RPMI 1640 containing 10% FCS, 600 μg/ml glutamine, 200 IU/ml penicillin, and 100 μg/ml streptomycin [Life Technologies]). The cells were differentiated into macrophage-like cells by the addition of 150 nM PMA (Sigma-Aldrich) 16–20 h prior to use in experiments.

Short hairpin RNA–mediated silencing

The lentiviral short hairpin RNA (shRNA) expression plasmid pLKO.1 was used for generating stable gene expression knockdown in THP1 cells (Open Biosystems, Huntsville, AL). The targeting shRNA sequence was IFI16 clone TCRN0000019079, Sting clone TCRN000163296, and AIM2 clone TRCN0000107503. The control shRNA vector was an empty vector pLKO.1 with an 18-nt shuttle sequence instead of the hairpin sequences. Virus-like particles were produced using Fugene 6 (Roche) transfection of HEK293T cells with the packaging system pMDIg/p-RRE, pRSV-rev,

pMG.2, and shRNA vector plasmid. Virus supernatants were harvested after 48 h and filtered through a 0.45-μm membrane. Undifferentiated THP1 cells were infected with increasing amounts of virus supernatant and placed under selection by adding 1 μg/ml puromycin 2 d postinfection. Levels of knockdown on IFI16 and STING were determined by Western blotting on extracts from differentiated THP1 cells, as described (27). For detection of AIM2, we used anti-human AIM2 (Adipogen; clone 3B10) and anti–β-actin.

Murine intranasal MHV68 infection model

Mice were infected intranasally with 5×10^4 PFU MHV68 in 25 μl while under anesthesia. On day 3, 6, 16, or 90 postinfection, the mice were euthanized by cervical dislocation and used for further analysis.

Isolation of single cells from the lung

The lungs were removed and tissue injected with 1 ml digestion media (1 mg/ml collagenase/dispase, 0.5 mg/ml DNase in PBS), followed by digestion in a medium of IMEM, 10% FCS, 1 mg/ml collagenase/dispase, and 0.5 mg/ml DNase for 30 min at 37 °C. Single cells of the lungs were then obtained by grinding the tissues and passing them through a 70 μm strainer. The cell suspension was incubated with ACK lysis buffer for 3 min to eliminate the RBCs and then washed and the supernatant discarded. Single cells were resuspended in 0.5% BSA/PBS for subsequent analysis.

Flow cytometry analysis

Single cells were blocked with Fc-blocking Ab (2.4G2) and subsequently stained with the following Abs: CD11b (M1/70), Ly6g (1A8), CD3 (17A2), CD19 (1D3), I-Ab (AF6-120.1) and CD11c (HL3) (all from BD); CD4 (GK1.5) and CD8a (53-6.7) (both from eBioscience); and F4/80 (Cl:A3-1; Serotec). Dead cells were excluded by staining with Aqua (Invitrogen). Data were collected with an FC500 instrument (Beckman Coulter) and analyzed using FlowJo software (TreeStar).

Gene expression analysis by nCounter

RNA was isolated from cells that were mock infected or infected with MCMV and MHV68, as indicated. Cells were harvested into RLT buffer containing 2-ME for subsequent processing with the RNeasy Mini kit (QIAGEN). Each RNA sample was adjusted to contain the same quantity using the Nanodrop ND-1000 spectrophotometer (Thermo Scientific). RNA was hybridized and quantified with the nCounter Analysis System (NanoString Technologies, Seattle, WA) using a customized probe set containing probes for innate immune genes, per the manufacturer's protocol. The gene expression data were normalized to an internal positive control, then to an internal negative control, and, finally, to seven housekeeping genes: GAPDH, β-glucuronidase, β-actin, hypoxanthine phosphoribosyltransferase 1, tubulin β, phosphoglycerate kinase 1, and clathrin H chain 1. All values were log10 transformed, and a heat map was generated using the open source R-based software at the University of Massachusetts Medical School.

ELISA

Supernatants or spleen homogenates from cell cultures and mice, respectively, were analyzed for cytokine levels by ELISAs for human IL-1β and the murine cytokines IL-1β, CXCL10, TNF-α, IFN-γ, and IL-6 using matched Ab pairs obtained from R&D Systems, as described previously (17, 28).

Type I IFN bioassay

IFN-α/β levels were measured by a cell-based assay. In brief, supernatants harvested from BMDCs or BMMs were UV treated for 6 min to inactivate residual virus in the samples. Then samples were plated in successive 2-fold dilutions on a 96-well plate, with 20,000 L929 cells/well, in 100 μl MEM with 5% FCS. After overnight incubation, the L929 cells were infected with vesicular stomatitis virus (VSV/V10). After 2–3 d of infection, the cells in each well were examined with a microscope. A 50% protection of cells from virus-induced cell death in a well was used to define 1 U/ml IFN-α/β.

Quantitative real-time PCR analysis

RNA was purified from homogenates of lung tissues using an RNeasy Plus Mini Kit (QIAGEN), following the manufacturer's protocol. The RNA was treated with DNase I to eliminate contaminating genomic DNA. RNA was isolated from cells in culture using a High Pure RNA Isolation Kit (Roche). Expression or mRNAs for human and murine cytokines were determined by real-time PCR, using TaqMan detection systems (Applied Biosystems). Expression levels were normalized to β-actin expression, and data are presented as the fold induction over untreated controls for each phenotype. The TaqMan assays used were hIFN-β, Hs01077958_s1; hTNF-α, Hs01113624_g1; hβ-actin Hs99999903_m1; mIFN-β, Mm00439546_s1; mCXCL10, Mm00445235_m1; and mβ-actin, Mm01205647_g1. For detection of viral genomic material, DNA was isolated from lungs and spleens using an ISOLATE II Genomic DNA Kit (Bioline). For amplification of MHV68 glycoprotein B DNA we used the following primers: forward: 5′-CCGCTCATTACGGCCCAAATTCAA-3′ and reverse: 5′-GGCAGCGACAGGCTTTCCATAAAT-3′. SYBR Green was used as a fluorescent dye to quantitate DNA products in real time.

Confocal microscopy

For visualization of IFI16 and STING following infection, THP1 cells were fixed and permeabilized with methanol at −20°C and labeled with Abs against IFI16 (N-terminal Santa Cruz sc-8023) or STING (Imgenex IMG-6485A). Images were acquired on a Zeiss LSM 710 confocal microscope using a 63× 1.4 oil-immersion lens. Image processing was performed using Zen 2010 (Zeiss) and ImageJ.

Propagation of deoxy-5-ethynylcytidine–labeled MHV68 and visualization of capsid-free DNA

Deoxy-5-ethynylcytidine (EdC)-labeled MHV68 was propagated in BHK-21 cells in the presence of 3 μM EdC (Sigma-Aldrich), which was added at 6 h post infection. The supernatant was collected 4 d later, and debris was removed by centrifugation at 4500 × *g* for 1 h. Virus in the supernatant was pelleted at 26,700 × *g* for 5 h and resuspended in PBS, followed by determination of the viral titers on BHK-1 cells. The Click-iT Imaging Kit (Invitrogen) was used to visualize capsid-free viral DNA in the infected cells. Briefly, the infected cells were fixed with methanol for 5 min at −20°C and stained with click staining mix, freshly prepared according to the manufacturer, at room temperature for 30 min in the dark. Nucleoli of the cells were stained with DAPI. Images were acquired on a Zeiss LSM 710 confocal microscope, using a 63× 1.4 oil-immersion objective, and image processing was performed using Zen 2010 (Zeiss).

Statistics

Data are shown as mean ± SD. A statistically significant difference between observations was determined using the two-tailed Student *t* test or Wilcoxon rank-sum test. For p values < 0.05, differences were considered statistically significant.

Ethics

Protocols for the animal experiments were approved by the Local Ethical committees and conducted in accordance with institutional guidelines for animal care and use.

Results

Induction of innate immune responses by α-, β-, and γ-herpesviruses in leukocytes

In a first series of experiments, we wanted to characterize the ability of MHV68 to induce cytokines associated with innate immune responses and compare with MCMV and HSV-1. BMDCs were seeded and infected with increasing doses of MHV68, HSV-1, and MCMV. The doses of MCMV and HSV-1 were chosen based on experiments in which CXCL10 induction by different doses of these viruses was examined (Supplemental Fig. 1A). Despite clear induction of type I IFN expression by MCMV and HSV-1 infections, we were not able to detect IFN bioactivity in the supernatants from cells infected with MHV68 (Fig. 1A). This was not due to lack of infection of the cells, as measured by expression of GFP in cells infected with an MHV68-GFP virus (Supplemental Fig. 1B). In contrast to the lack of type I IFN induction, MHV68 infection in DCs stimulated the expression of TNF-α, IL-6, and IL-1β, although high doses of virus were required (Fig. 1B–D). Similar results were observed in BMMs, with no detectable IFN bioactivity in the supernatants from MHV68-infected cells but clear induction of IL-6 and TNF-α and modest induction of IL-1β (Supplemental Fig. 1C–F).

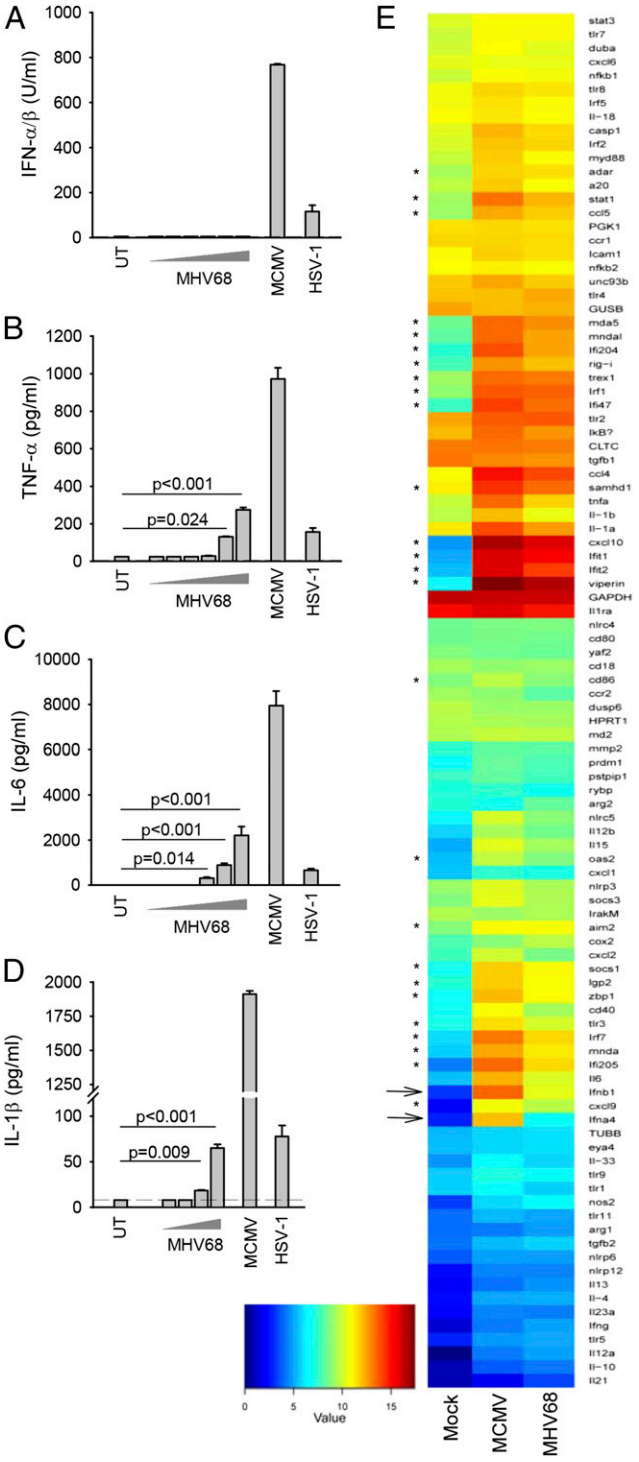

FIGURE 1. MHV68 stimulates a blunted innate immune response in DCs. (**A**–**D**) Mouse BMDCs from C57BL/6 mice were seeded and infected with increasing doses of MHV68 [MOI between 1 and 1000; MOI between 10 and 100 in (D)], MCMV (MOI 1), or HSV-1 (MOI 3). Supernatants were harvested 24 h postinfection and used for measurement of cytokines by type I IFN bioassay (A) or ELISA (B–D). Data are means (± SD) of measurements from triplicate cultures. (**E**) BMDCs were treated with MCMV (MOI 10) and MHV68 (MOI 10) for 6 h prior to harvest of total RNA, which was subjected to analysis for specific transcripts using NanoString Technology. Data are presented as heat maps. Arrows indicate type I IFN genes, and stars indicate IFN-stimulated genes. Data are representative of three independent experiments.

To get a more complete picture of the innate response evoked by MHV68 infection in DCs, we subjected RNA isolated from mock or virus-infected cells to analysis using nCounter (NanoString Technologies), a fluorescent barcoded technique that allows multiplex analysis of mRNAs important in innate immunity. Infection with MHV68 stimulated expression of most mRNA transcripts for which we tested (Fig. 1E). However, the response to MHV68 infection was generally much lower than that induced by MCMV infection. In particular, transcripts for type I IFNs (IFN-β and IFN-α4) and IFN-stimulated genes accumulated at much lower levels in cells infected with MHV68 compared with MCMV. Consistent with this, we found induction of the IFN-stimulated gene CXCL10 at the protein level only after MHV68 infection at a high multiplicity of infection (MOI) (Supplemental Fig. 1G).

Altogether, infection of macrophages and DCs with the gammaherpesvirus MHV68 induced expression of genes associated with innate immunity to a limited extent compared with infection with other classes of herpesviruses. In particular, the IFN response to MHV68 infection was weak, indicating that this virus possesses immune-evasion strategies targeting the IFN pathway.

Role for TLRs and DNA-sensing pathways in the innate immune response to herpesviruses in DCs

To characterize the pathways through which herpesviruses induced innate immune responses, we first examined whether lack of STING expression affected activation of innate immune responses by MHV68. For comparison, we included α- and β-herpesviruses in the analysis. As expected, induction of type I IFN bioactivity by HSV-1 and MCMV was strongly reduced in cells from STING$^{gt/gt}$ mice (Fig. 2A-i, 2B-i), whereas the IL-1β response was not affected (Fig. 2A-ii, 2B-ii). In addition, the induction of TNF-α and IL-6 by the α- and β-herpesviruses was significantly impaired in BMDCs lacking STING (Fig. 2A-iii, 2A-iv, 2B-iii, 2B-iv), clearly demonstrating an essential role for STING in immune activation beyond the IFN pathway. In sharp contrast to the strong dependence on STING for induction of innate immune responses by HSV-1 and MCMV, we found that the ability of MHV68 to evoke expression of TNF-α and IL-6 was not affected by the absence of STING (Fig. 2C), but it was significantly compromised in cells from TLR2/9$^{-/-}$ mice (Supplemental Fig. 2A–D). As controls we measured cytokine levels in supernatants from BMDCs treated with synthetic dsDNA or poly I:C. These data confirmed an essential role for STING in DNA-induced expression of type I IFNs, IL-6, and TNF-α but not IL-1β (Fig. 2D) and that RNA-induced innate immune responses occur independently of STING (Fig. 2E). Collectively, these data show that MHV68 stimulates expression of inflammatory cytokines in myeloid cells in a manner independent of STING but dependent on TLRs.

In a next series of experiments, we challenged mice intranasally with MHV68 and examined viral load in the lungs during the acute phase of the infection (days 3 and 6) and in the spleen during latency (days 16 and 90). Interestingly, we observed elevated levels of viral DNA in the lungs of STING$^{gt/gt}$ mice on day 3 postinfection (Fig. 2F); however, this difference did not reach statistical significance on day 6 postinfection (Fig. 2G). On days 16 and 90, no significant difference in splenic latent viral load was observed between C57BL/6 and STING$^{gt/gt}$ mice (Fig. 2H, 2I). In agreement with this, STING-deficient mice exhibited an early weight loss after MHV68 infection that was not seen in WT mice, but at later time points the two mice strains followed indistinguishable weight curves (Fig. 2J). Flow cytometric characterization of spleen cells from C57BL/6 and STING$^{gt/gt}$ mice revealed no significant difference in the number of B cells between the two strains (Table I). B cells are required for establishment of latency

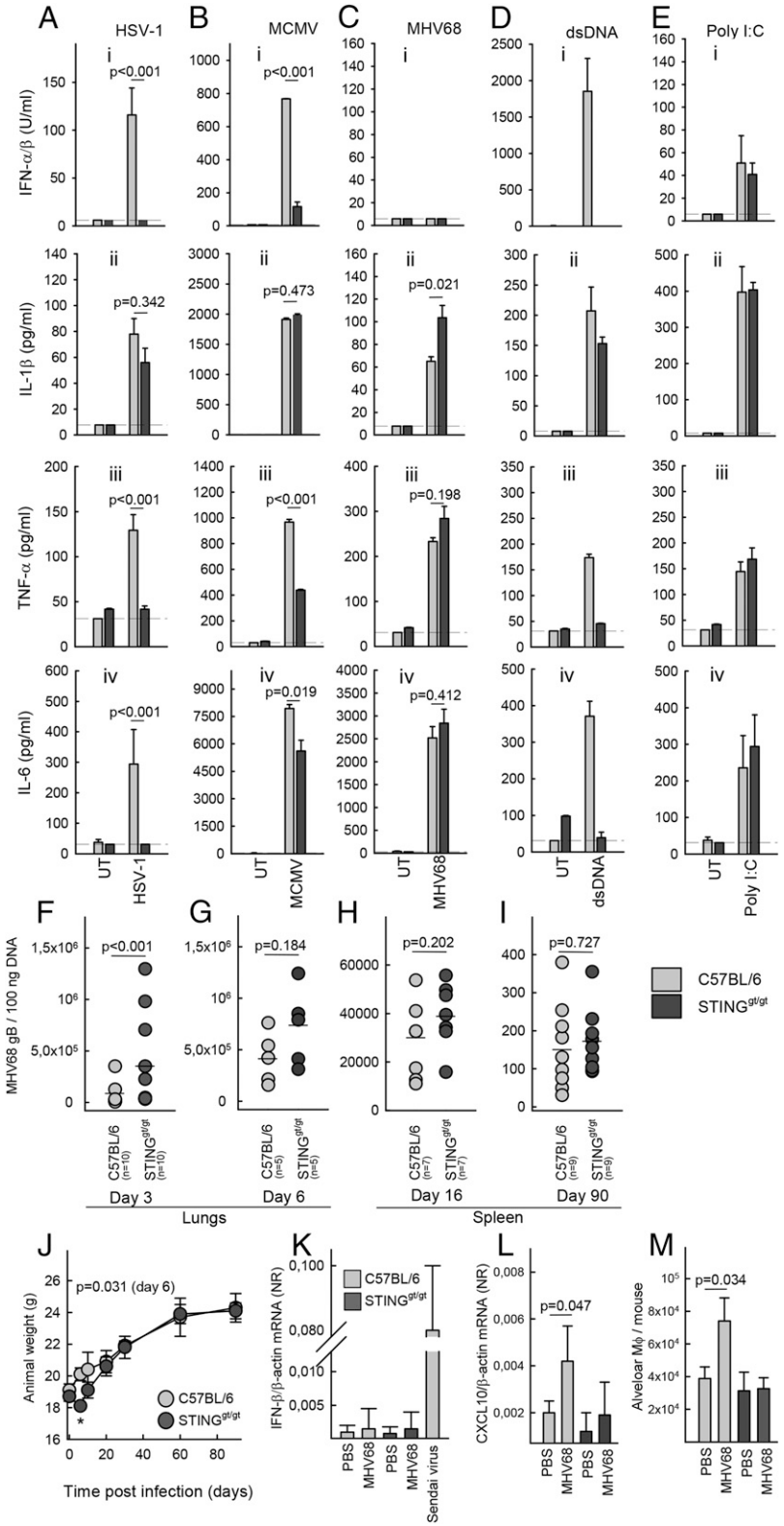

FIGURE 2. A limited role for STING in host control of MHV68 infection. BMDCs from C57BL/6 and STING$^{gt/gt}$ mice were treated with HSV-1 (MOI 3) (**A**), MCMV (MOI 3) (**B**), MHV68 (MOI 100) (**C**), dsDNA (2 μg/ml) (**D**), or poly I:C (**E**). Supernatants were harvested 18 h posttreatment for measurement of type I IFN bioactivity (A**i**–E**i**), IL-1β (A**ii**–E**ii**), TNF-α (A**iii**–E**iii**), and IL-6 (A**iv**–E**iv**). Data are mean (± SD) from triplicate cultures and are representative of three independent experiments. (**F**–**I**) C57BL/6 and STING$^{gt/gt}$ mice were infected intranasally with 5×10^4 PFU of MHV68. Lungs were isolated from mice infected for 3 d (F) or 6 d (G), and spleens were isolated from mice infected for 16 d (H) or 90 d (I). Organs were homogenized and analyzed for the presence of MHV68 DNA by PCR. Each symbol represents an individual mouse. (**J**) Weights of C57BL/6 and STING$^{gt/gt}$ mice infected with MHV68. Data are mean ± SD for each group of animals. A statistically significant difference between C57BL/6 and STING$^{gt/gt}$ mice on day 6 is indicated by a star, and the *p* value is given. (**K** and **L**) RNA was isolated from lung homogenates from C57BL/6 and STING$^{gt/gt}$ mice (n = 5 mice/group) 3 d after intranasal treatment with PBS or MHV68 (5×10^4 PFU) and analyzed for levels of IFN-β and CXCL10 mRNA by quantitative real-time PCR. Data are mean ± SD. (**M**) Single-cell suspensions from lungs of C57BL/6 and STING$^{gt/gt}$ mice (n = 5 mice/group) treated for 3 d as in (J) and (K) and analyzed by flow cytometry for levels of macrophages using CD45$^+$ autofluorescence$^+$ CD11b^{low} CD11c$^+$ as markers. Data are mean (± SD) number of alveolar macrophages/mouse.

after intranasal MHV68 infection (29); however, we observed that several leukocyte cell types were suppressed in STING$^{gt/gt}$ mice, but not in C56BL/6 mice, infected with MHV68 for 90 d (Table I). For TLR2/9$^{-/-}$ mice, we also observed elevated viral load in the lungs on day 3 but not in the spleen on day 90 (Supplemental Fig. 2E, 2F). Despite the early STING-dependent control of MHV68 in the lungs, we did not find elevated expression of IFN-β mRNA in the lungs of infected mice (Fig. 2K). By performing a wider screen for MHV68-induced gene expression in the lungs, CXCL10 was the only mRNA found to be elevated in the lungs postinfection, and this was dependent on expression of STING (Fig. 2L). This correlated with early recruitment of macrophages to the lungs through a STING-dependent process (Fig. 2M). Thus, STING plays a limited role in activation of the pathways mediating control of MHV68, which failed to induce type I IFN responses in vitro and in vivo; however, we observed a very early role for

Table I. Flow cytometric characterization of spleens from C57BL/6 and STING$^{gt/gt}$ mice after MHV68 infection

	WT		STING$^{gt/gt}$	
	PBS (n = 5)	MHV68 (n = 9)	PBS (n = 6)	MHV68 (n = 7)
Total splenocytes	156.2 ± 12.5	189.50 ± 11.1*	126.8 ± 22.4	98.8 ± 5.7
CD11c$^+$	5.8 ± 0.6	5.60 ± 0.5	4.2 ± 0.5	2.8 ± 0.2*
CD11b$^+$CD11c$^+$	3.5 ± 0.5	3.15 ± 0.4	2.4 ± 0.3	1.5 ± 0.1*
I-Ab$^+$ in CD11c$^+$	3.1 ± 5.9	2.60 ± 4.2	2.1 ± 0.3	1.3 ± 0.2*
CD11b$^+$CD11c$^-$	14.1 ± 1.1	13.50 ± 1.8	10.2 ± 2.7	5.1 ± 0.7
CD19$^+$	72.1 ± 10.7	82.90 ± 6.5	61.6 ± 7.5	60.7 ± 2.9
CD3$^+$	46.0 ± 3.0	56.10 ± 5.7	43.8 ± 4.1	33.6 ± 3.2*
F4/80$^+$	1.6 ± 0.5	14.90 ± 6.6*	1.5 ± 0.2	1.6 ± 7.2

Data are mean (± SD) cell numbers ($\times 10^6$).
*$p < 0.05$, versus PBS.

STING in vivo, correlating with low induction of CXCL10 and recruitment of macrophages.

The finding that MHV68-induced cytokine expression occurred independently of STING indicated that this virus, in contrast to α- and β-herpesviruses, triggers innate immune responses independent of intracellular DNA sensing. The AIM2 inflammasome pathway is another major pathway of DNA-driven innate immune activation. Therefore, we examined the role of AIM2 in production of IL-1β in LPS-primed BMMs. We first showed that these cells produced high amounts of IL-1β in response to the potent inflammasome activator poly(dA:dT), and this was dependent on AIM2 and the inflammasome adaptor protein ASC but not NLRP3 (Fig. 3A). For MCMV, production of IL-1β was strongly reduced in AIM2$^{-/-}$ and ASC$^{-/-}$ cells, as previously reported (4) (Fig. 3A). In contrast, MHV68 induced IL-1β secretion in a manner independent of AIM2 but dependent on NLRP3 and ASC (Fig. 3B). The AIM2-independent nature of the MHV68-driven response also was observed in vivo, because AIM2 deficiency did not reduce the levels of IL-1β or IFN-γ, the latter produced through an IL-18–dependent pathway (4), in mice infected with MHV68 (Fig. 3C, 3D). In further support of the lack of a role for AIM2 in immune sensing of MHV68, AIM2 deficiency did not affect viral load in mice latently infected with MHV68 (Fig. 3E). In contrast, ASC$^{-/-}$ and NLRP3$^{-/-}$ mice exhibited significantly elevated viral load, demonstrating that the inflammasome was involved in control of MHV68 infection (Fig. 3E). Collectively, these data demonstrate that MHV68 activates the inflammasome pathway via the NLRP3-ASC pathway and independently of the DNA-sensing AIM2 inflammasome.

KSHV induces innate immune responses independently of known DNA-stimulated pathways

KSHV is a human gammaherpesvirus closely related to MHV68 and the cause of Kaposi's sarcoma (30). To determine whether KSHV also stimulates innate immune responses independently of known intracellular-sensing systems, we first examined the effect of STING knock-down on virus-induced cytokine expression. The STING shRNA knock-down cell line was reported previously (27) and was tested to have >80% reduced expression of STING compared with the empty vector control cell line. As shown in Fig. 4A and 4B, knock-down of STING in THP1 cells reduced expression of IFN-β and TNF-α induced by HSV-1 or dsDNA, but it did not affect the cytokine response to KSHV. This was not due to the inability of KSHV to infect the cells, as evidenced by green fluorescence in cells infected with a GFP-encoding KSHV (Supplemental Fig. 3). Consistent with a limited role for STING in the response to KSHV, we found that, in contrast to what was observed after human CMV infection, neither STING nor IFI16 was mobilized postinfection with this virus (Fig. 4C). To test the role of AIM2 in KSHV-induced IL-1β expression, we generated a stable THP1 cell with shRNA-mediated knock-down of AIM2 (Fig. 4D). However, despite efficient knock-down of AIM2, the ability of KSHV to induce IL-1β production was not affected. It was reported that KSHV activates an IFI16-dependent inflammasome after nuclear sensing of the virus in endothelial cells (14). To test the role of IFI16 in IL-1β production during KSHV infection, we measured IL-1β levels in supernatants from THP1 cells expressing control shRNA or IFI16 shRNA. The IFI16 shRNA knock-down cell line was reported previously (27) and was tested to have >80% reduced expression of IFI16 compared with the empty vector control cell line. In contrast to the previous data from endothelial cells, we did not observe reduced KSHV-induced IL-1β expression in monocytic cells with IFI16 knock-down (Fig. 4E). We also found that the induction of IFN-β by KSHV was independent of IFI16, in contrast to HSV-1, which relied on this DNA sensor for stimulation of IFN-β expression, as previously reported (17). Altogether, these data show that KSHV, like MHV68, stimulates innate immune responses independently of the DNA-driven pathways via STING and AIM2.

The MHV68 ORF64 DUB antagonizes innate immune responses activated by viral DNA

Given the finding that MHV68 infection in myeloid cells did not lead to detectable innate immune activation by the DNA-sensing pathway, we were interested in identifying the step in the pathway targeted by the virus. In a first series of experiments, we pretreated murine DCs with MHV68, followed by infections and stimulations as indicated in Fig. 5A. Supernatants were collected for measurement of type I IFN activity. Interestingly, we observed that HSV-1–induced expression of type I IFN, CXCL10, and IL-6 was abrogated in cells pretreated with MHV68 (Fig. 5A, Supplemental Fig. 4A, 4B). In contrast, MHV68 infection did not affect the ability to activate the pathway via dsDNA or cGAMP nor was the virus able to modulate the intracellular RNA-sensing pathway. The inhibition of HSV-induced cytokine expression by MHV68 was not due to a blockage of HSV-1 entry, because accumulation of the HSV major capsid protein VP5 in the cytoplasm of infected cells was not affected by pretreatment with MHV68 (Supplemental Fig. 4C). Similar to the inhibition of HSV-1–induced IFN expression, MHV68 also inhibited IL-1β expression induced by MCMV but not synthetic DNA (Fig. 5B). Upon examination of the assembly of STING signalsomes, as measured by STING foci formation and recruitment of Tank-binding kinase-1 (TBK1), we found that, although HSV-1 infection stimulated this activity, MHV68 infection did not (Fig. 5C). Despite the lack of

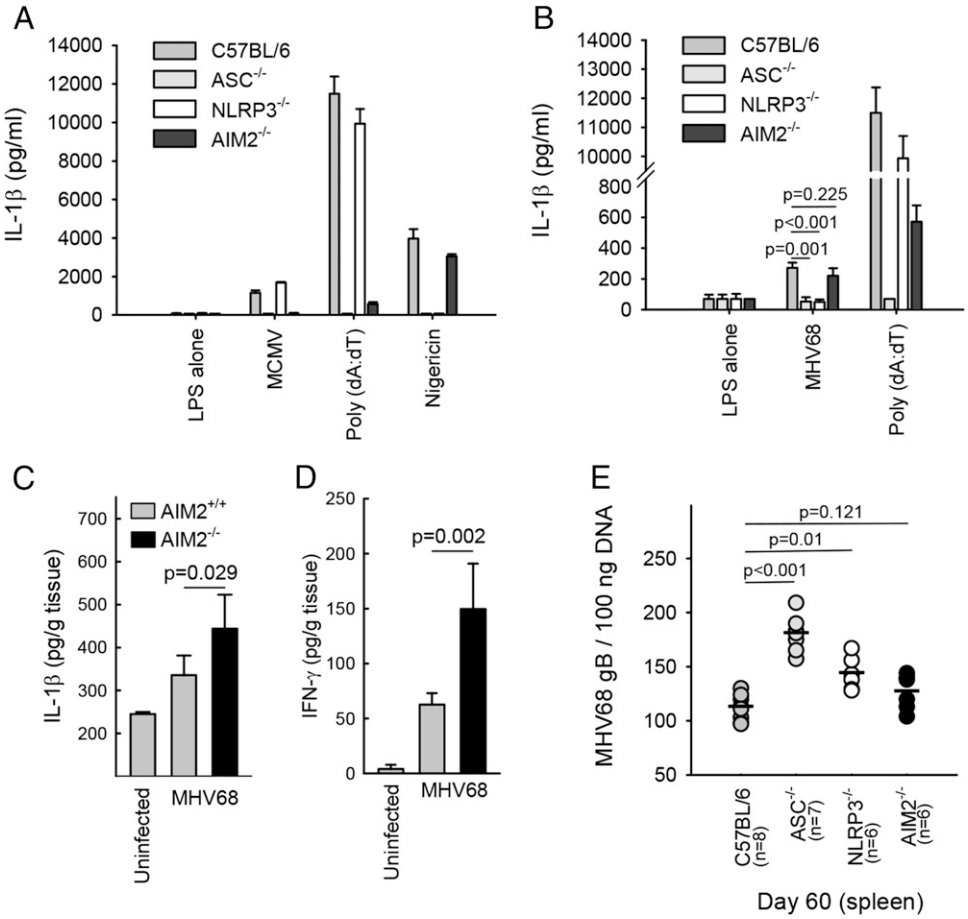

FIGURE 3. The AIM2 inflammasome is not involved in immune activation during MHV68 infection. (**A** and **B**) BMMs from C57BL/6, ASC$^{-/-}$, NLRP3$^{-/-}$, and AIM2$^{-/-}$ mice were stimulated with LPS (200 ng/ml) for 3 h prior to treatment with MCMV (MOI 10), poly(dA:dT) (1 μg/ml), nigericin (10 μM), or MHV68 (MOI 10). Supernatants were harvested 24 h posttreatment for measurement of IL-1β. Data are mean ± SD from triplicate cultures. (**C**–**E**) C57BL/6 and AIM2$^{-/-}$ mice were infected with 5×10^5 PFU of MHV68. Spleens were isolated from mice infected for 6 or 60 d, homogenized, and analyzed for levels of IL-1β and IFN-γ by ELISA (day 6) or for MHV68 DNA by PCR (day 60). ELISA data in (C) and (D) are means ± SD (n = 6–8 mice/group). In (E), each symbol represents an individual mouse. Data are representative of three independent experiments.

response to MHV68 infection, purified MHV68 DNA induced IFN-β expression if transfected into cells (Fig. 5D). These findings suggest that MHV68 infection inhibits herpesvirus-driven DNA-mediated immune activation and suggests that this occurs upstream of the bifurcation into the STING-dependent IFN pathway and the AIM2-dependent IL-1β pathway.

The findings above indicate that gammaherpesviruses target a step common for all virus-activated DNA-dependent innate pathways tested. We recently reported that α- and β-herpesvirus capsids become ubiquitinated and degraded in the cytoplasm in macrophages, hence exposing the viral DNA to cytosolic DNA sensors (17). Because herpesviruses encode a conserved DUB activity embedded in the large tegument protein (21, 31, 32), we hypothesized that herpesviruses use this activity to counteract DNA-driven innate immune activation. To address this question, DCs were stimulated with a MHV68 mutant with a point mutation in the active site of the DUB, as well as with a revertant virus (21). Interestingly, in contrast to the revertant virus, infection with the DUB active site mutant virus did stimulate type IFN activity and led to elevated IL-1β production (Fig. 5E, 5F). The IFN response was dependent on STING, thus demonstrating that deletion of the DUB activity of ORF64 exposes an intrinsic capacity of gammaherpesviruses to stimulate DNA-driven innate immune responses (Fig. 5G). The MHV68 kinase ORF36, previously reported to inhibit IFN regulatory factor 3 activation in fibroblasts (22), did not seem to be essential for evasion of DNA-driven IFN expression in myeloid cells (Supplemental Fig. 4D). To evaluate whether infection with the ORF64 C33A mutant differed from WT virus with respect to subcellular localization of viral genomes, we generated MHV68 with EdC incorporated into the viral genomes. In infected cells the viral genomes were visualized using click chemistry (33). Interestingly, although the viral genome was found mainly in the nucleus of cells infected with the revertant virus, viral DNA was localized preferentially in the cytoplasm in cells infected with the ORF64 C33A virus (Fig. 5H, 5I).

To evaluate whether the DUB activity of α- and β-herpesviruses also plays a role in immune evasion, DCs were infected with WT or DUB mutant HSV-1 and MCMV, followed by measurement of IFN bioactivity in the culture supernatants. For both HSV-1 and MCMV, we found that, although the WT viruses induced IFN expression, this was elevated further in the absence of the tegument DUB activity (Fig. 5J, 5K). Together, these data demonstrate that deletion of the DUB activity of the large MHV68 tegument protein ORF64 leads to augmented cytosolic localization of viral DNA and renders MHV68 capable of stimulating DNA-driven innate immune responses. Moreover, the data also reveal the herpesvirus tegument DUB activity to be a conserved mechanism

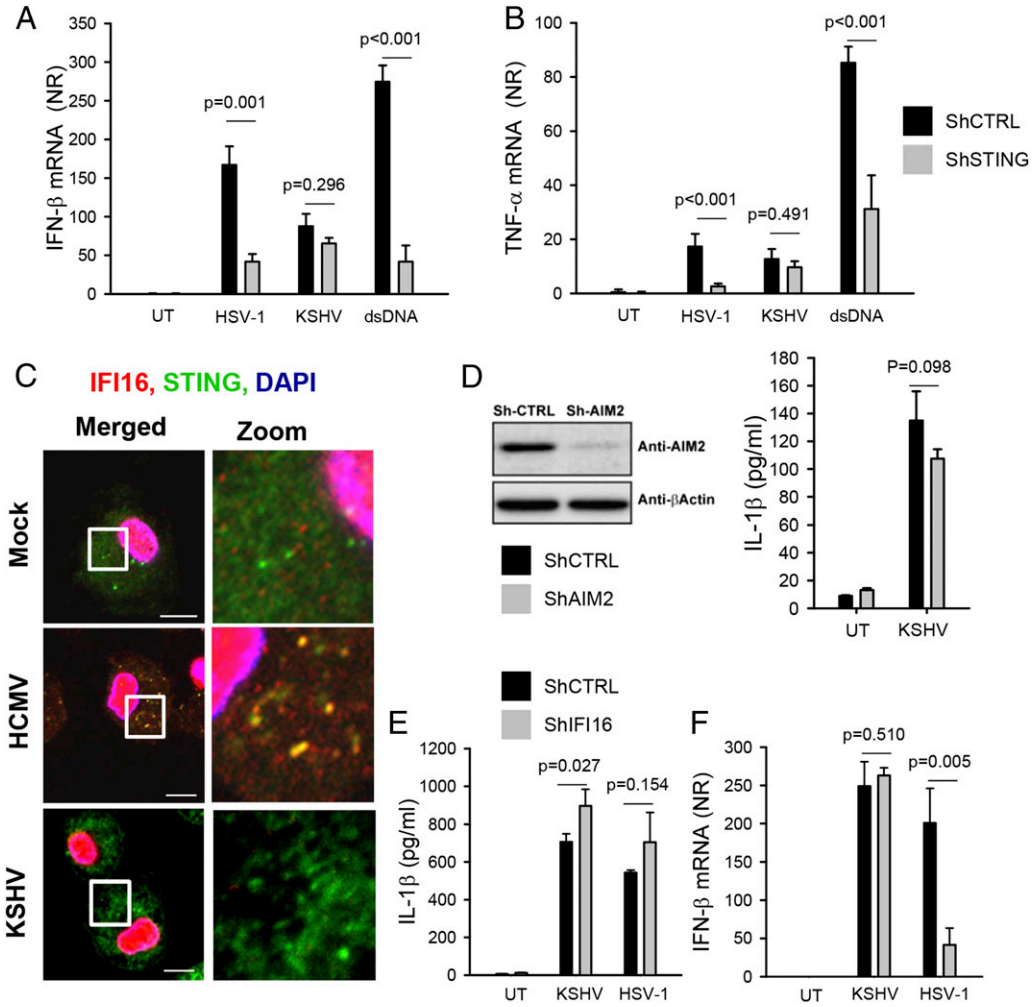

FIGURE 4. KSHV induces expression of IFN-β and production of IL-1β independent of the STING and AIM2 pathways. (**A** and **B**) PMA-differentiated THP1-derived cells stably transduced with lentiviral shRNAs (control and STING) were infected with HSV-1 (MOI 3) or KSHV (30 genomes/cell) or transfected with dsDNA (2 μg/ml). Total RNA was harvested 6 h posttreatment and analyzed for levels of IFN-β and TNF-α. Data are means (± SD) of normalized ratios relative to untreated, using β-actin as internal reference. (**C**) Monocyte-derived macrophages were infected with CMV (MOI 3) or KSHV (30 genomes/cell) for 4 h. Subcellular distribution of IFI16 and STING was assessed by confocal microscopy. White box indicates area displayed in Zoom column (original magnification ×5). Scale bars, 10 μm. (**D**) Western blot of AIM2 and β-actin on extracts from PMA-differentiated THP1-derived cells stably transduced with lentiviral shRNAs (control and AIM2). The shRNA THP1 cells were left untreated or infected with KSHV. Supernatants were harvested 18 h posttreatment, and levels of IL-1β were measured by ELISA. Data are means (± SD) of normalized ratios relative to untreated. (**E** and **F**) PMA-differentiated THP1-derived cells stably transduced with lentiviral shRNAs (control and IFI16) were infected with HSV-1 (MOI 3) or KSHV (30 genomes/cell). Total RNA and culture supernatants were harvested 6 and 18 h posttreatment, respectively, and analyzed for levels of IFN-β mRNA and IL-1β protein. Data are mean (± SD) normalized ratios (NR) relative to untreated. All data are representative of four or more independent experiments.

to counteract immune activation through the DNA-driven STING pathway.

ORF64 DUB deficiency enables a STING-dependent antiviral pathway controlling establishment of a latent MHV68 reservoir

Given the finding that the ORF64 DUB active site mutant gained the capacity to induce IFN expression in a STING-dependent manner, we were interested in examining whether this MHV68 mutant had an altered course of infection in WT and $STING^{gt/gt}$ mice. A previous report has shown that the MHV68 ORF64 C33A mutant was not attenuated with respect to the ability to establish latent infection after i.p. infection (21). In this study, we used the intranasal infection model, and it was reported previously that the route of infection affects the role of innate immune pathways in control of MHV68 infection (19). We first examined whether the MHV68 ORF64 DUB mutant was capable of inducing IFN-β expression in vivo and also whether treatment with rIFN-β affected the acute viral load in the lungs and the latent viral reservoir in the spleen. As shown in Fig. 6A, RNA in lung homogenates from mice infected for 3 d with the MHV68 ORF64 C33A mutant contained elevated levels of IFN-β mRNA, whereas IFN-β mRNA levels in homogenates from mice infected with the revertant virus were indistinguishable from the mock-treated mice. This finding prompted us to evaluate whether an elevated innate immune response could affect viral load in infected organs at different time points during the infection. Therefore, mice were treated with rIFN-β and rTNF-α before the infection and once every week during the course of the infection. When evaluating the viral load in the lungs, we found that IFN-β treatment led to reduced accumulation of viral DNA on day 6 postinfection (Fig. 6B). Interestingly, in the spleens harvested 90 d postinfection, treatments with single cytokines did not affect the latent viral load, whereas this was the case in spleens from mice treated with both IFN-β and TNF-α (Fig. 6C). Thus, the elevated expression of proteins

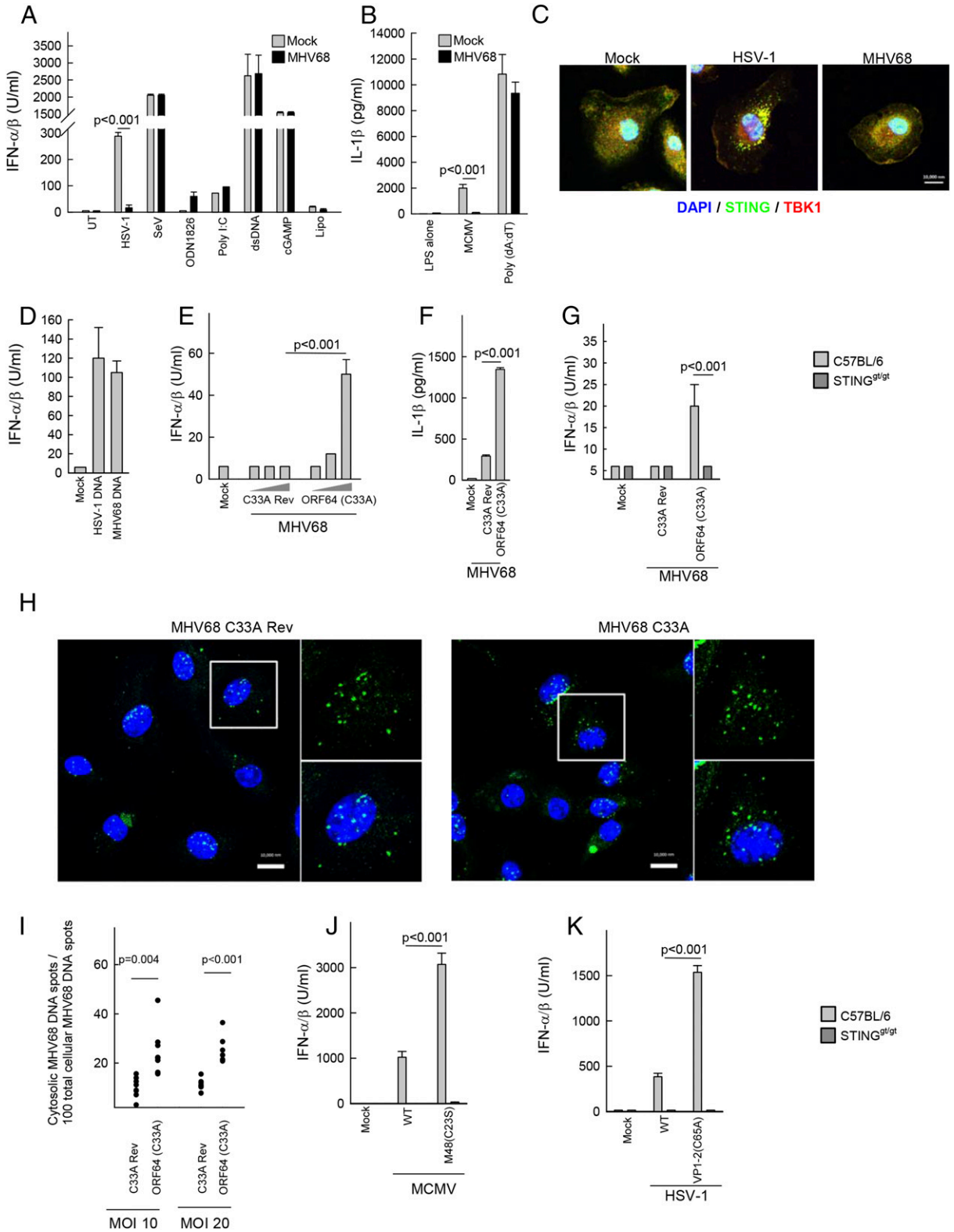

FIGURE 5. The DUB activity of MHV68 mediates evasion of herpesvirus-induced production of type I IFN and IL-1β. (**A** and **B**) BMDCs from C57BL/6 mice were infected with MHV68 (MOI 10) 1 h prior to treatment with HSV-1 (MOI 3), MCMV (MOI 1), ODN1826 (1 μM), poly I:C (25 μg/ml), dsDNA (2 μg/ml), cGAMP (2 μM), or Lipofectamine. Supernatants were harvested 16 h later for measurement of type I IFN bioactivity and IL-1β. (**C**) BMDCs from C57BL/6 mice were infected with HSV-1 (MOI 3) and MHV68 (MOI 20) for 5 h and stained with DAPI and anti-STING and anti-TBK1 Abs. Scale bar, 10 μm. (**D**) BMDCs were stimulated with genomic DNA from HSV-1 and MHV68 (0.25 μg/ml). Supernatants were isolated 18 h poststimulation for measurement of IFN bioactivity. (**E** and **F**) BMDCs from C57BL/6 mice were treated with MHV68 ORF64 C33A or the revertant virus at an MOI of 1, 10, and 100. Supernatants were harvested 16 h later for measurement of type I IFN bioactivity and IL-1β (only MOI 10). (**G**) BMDCs from C57BL/6 and STING$^{gt/gt}$ mice were infected with MHV68 ORF64 C33A or the revertant virus (MOI 50). Supernatants were harvested 18 h postinfection, and IFN bioactivity was measured. (**H**) BMMs were infected with EdC-labeled MHV68 ORF64 C33A or the revertant virus (MOI 20) for 3 h and fixed. Accessible DNA was visualized using copper(I)-catalyzed Azide Alkyne Cycloaddition staining. Nucleic acids were visualized using DAPI. (*Figure legend continues*)

associated with innate immune responses during infection with the MHV68 ORF64 DUB mutant could potentially affect viral load in the lung and the spleen.

In a final series of experiments, we challenged C57BL/6 and STING$^{gt/gt}$ mice with the MHV68 ORF64 C33A mutant or the revertant virus. When measuring viral load in the lung on day 3 postinfection, significantly elevated levels of virus were found in STING$^{gt/gt}$ mice compared with WT mice postinfection with either virus (Fig. 6D). However, no significant difference between the viral loads in the lungs of mice infected with the DUB mutant or revertant viruses was observed, regardless of the mouse strain (Fig. 6D). Thus, lack of ORF64 DUB activity does not affect the early stages of MHV68 infection. In contrast, when we looked for viral DNA in the spleen from mice infected for 16 or 90 d, we observed significantly lower levels in C57BL/6 mice infected with the MHV68 ORF64 DUB mutant compared with the revertant virus (Fig. 6E, 6F). Interestingly, the impaired ability of the MHV68 ORF64 DUB mutant to establish latent infection was rescued when the infection occurred in STING$^{gt/gt}$ mice. Similar experiments in TLR2/9$^{-/-}$ mice revealed that the ORF64 DUB mutation did not confer a mouse genetics–dependent differential latent viral load in this model (Supplemental Fig. 2G, 2H). Altogether, MHV68 antagonizes the STING-dependent pathway stimulated by viral genomic DNA through a mechanism dependent on the DUB embedded in ORF64, and this facilitates establishment of a latent reservoir of MHV68.

Discussion

KSHV and EBV are important human pathogens and are among the small group of viruses capable of causing tumors (30). These viruses belong to the family of gammaherpesviruses and have the capacity to establish lifelong latent-recurrent infections. The ability of the host to control infections with herpesviruses is important for prevention of disease, as exemplified by the frequent development of Kaposi's sarcoma in individuals with AIDS (30). It is now known that herpesviruses are controlled by both the innate and adaptive immune systems; despite this, there is limited knowledge on how the innate immune system detects infections with gammaherpesviruses. Recently, much attention has been given to DNA as a major stimulator of innate immune responses (34), and it was reported that α-herpesviruses (HSV) and β-herpesviruses (CMV) are detected by the DNA-sensing machinery (4, 10, 17). At this stage, two major pathways of immune activation by DNA are known: DNA-induced IFN responses relying on the adaptor protein STING (2) and DNA-stimulated inflammasome activation occurring via AIM2 (16). In this article, we show that WT MHV68 is a poor inducer of innate immune responses, and the responses evoked by MHV68, as well as by KSHV, are independent of described intracellular DNA-sensing systems known to be essential for host detection of α- and β-herpesviruses. In line with this, STING$^{gt/gt}$ and AIM2$^{-/-}$ mice did not exhibit major defects in control of MHV68 infection; in particular, the establishment of latent viral reservoirs was not affected by defective DNA-sensing pathways. An MHV68 mutant with a point mutation in the tegument DUB ORF64, which is conserved among herpesviruses, induced significant type I IFN expression through a STING-dependent mechanism. Moreover, WT mice infected with the DUB mutant harbored a lower latent viral load than did mice infected with the revertant virus, but this impaired activity of the DUB mutant was rescued in STING$^{gt/gt}$ mice. We propose that gammaherpesviruses target the DNA-sensing system, and this contributes to the ability of this class of viruses to establish latent infections.

MHV68 did not stimulate detectable IFN bioactivity in myeloid cells, but it did stimulate expression of IL-1β, IL-6, and TNF-α to significant levels. However, the IL-1β response was independent of AIM2, but it was dependent on NLRP3 and ASC, and the induction of TNF-α and IL-6 was dependent on TLR2 and TLR9. This was in contrast to the responses evoked by HSV-1 and MCMV, for which important roles were ascribed to STING and AIM2 for induction of type I IFN expression and secretion of IL-1β, respectively. Similar to what we found with MHV68 in murine myeloid cells, the induction of IFN-β and IL-1β evoked by KSHV infection in a human monocytic cell line was independent of STING and AIM2. Thus, unlike α- and β-herpesviruses, gammaherpesviruses are detected independently of the intracellular DNA-sensing system, at least in the cell types tested, where the TLR pathway is particularly important for induction of inflammatory genes, as well as for early control of viral load in vivo. The role of TLRs in sensing gammaherpesviruses is in line with previous work demonstrating that TLR2 and TLR9 can recognize gammaherpesviruses, with the recognition by TLR9 in plasmacytoid DCs being particularly well documented (9, 18, 19, 35). A role for TLR2 was reported in fibroblasts and in early control in the lung after intranasal MHV68 infection (35). It should be noted that we found elevated viral load in the lungs of STING$^{gt/gt}$ mice at early time points after MHV68 infection, correlating with weight loss and impaired recruitment of macrophages. We cannot explain this early phenotype, but possible explanations include activation of DNA sensing in cell types other than the ones examined in the current study, low-grade sensing of MHV68 DNA and activation of signaling in the myeloid cells at early time points, and activation of STING-dependent signaling independent of DNA sensing, such as virus–cell fusion (28). A recent study demonstrated modest elevation of MHV68 load in lungs and spleen of cGAS-deficient mice on day 7 after i.p. MHV68 infection (36). These results are consistent with our data, and suggest a minor role for the cGAS-STING pathway early during MHV68 infection, despite the presence of ORF64.

It was reported that KSHV and EBV can be sensed by IFI16 in the nucleus to stimulate an IFI16–ASC–caspase 1 inflammasome in permissive and latently infected cells (14, 37). In our system using a human monocytic cell line, we found that IFI16 was not essential for production of IL-1β during KSHV infection, indicating that this DNA sensor is not involved in KSHV-driven inflammasome activation in these cells. However, the data presented in this article do not address the question of where in the cell the DNA sensing takes place. Moreover, it is important to note that the proposed nuclear IFI16–ASC–caspase 1 inflammasome pathway is not abrogated in STING$^{gt/gt}$ or AIM2$^{-/-}$ mice. Therefore, a potential role for nuclear DNA sensing during herpesvirus infections is not excluded by our data.

The phenomenon of viral evasion of the innate immune response is well described and known to impact the pathogenicity of viruses

Scale bars, 10 μm. Original magnification ×4. The *bottom right panels* show the boxed regions at a higher magnification. The *upper right panels* show staining for the click reaction without DAPI. (**I**) Quantification of cytosolic MHV68 DNA versus total MHV68 genomes in BMMs infected for 3 h with EdC-labeled MHV68 ORF64 C33A or the revertant virus (MOI 10 and 20). BMDCs from C57BL/6 and STING$^{gt/gt}$ mice were infected with DUB active site mutants of MCMV (MOI 1) (**J**) and HSV-1 (MOI 3) (**K**). Supernatants were harvested 18 h postinfection, and IFN bioactivity was measured. All cytokine data are mean (± SD) from triplicate cultures. All data are representative of three or more independent experiments.

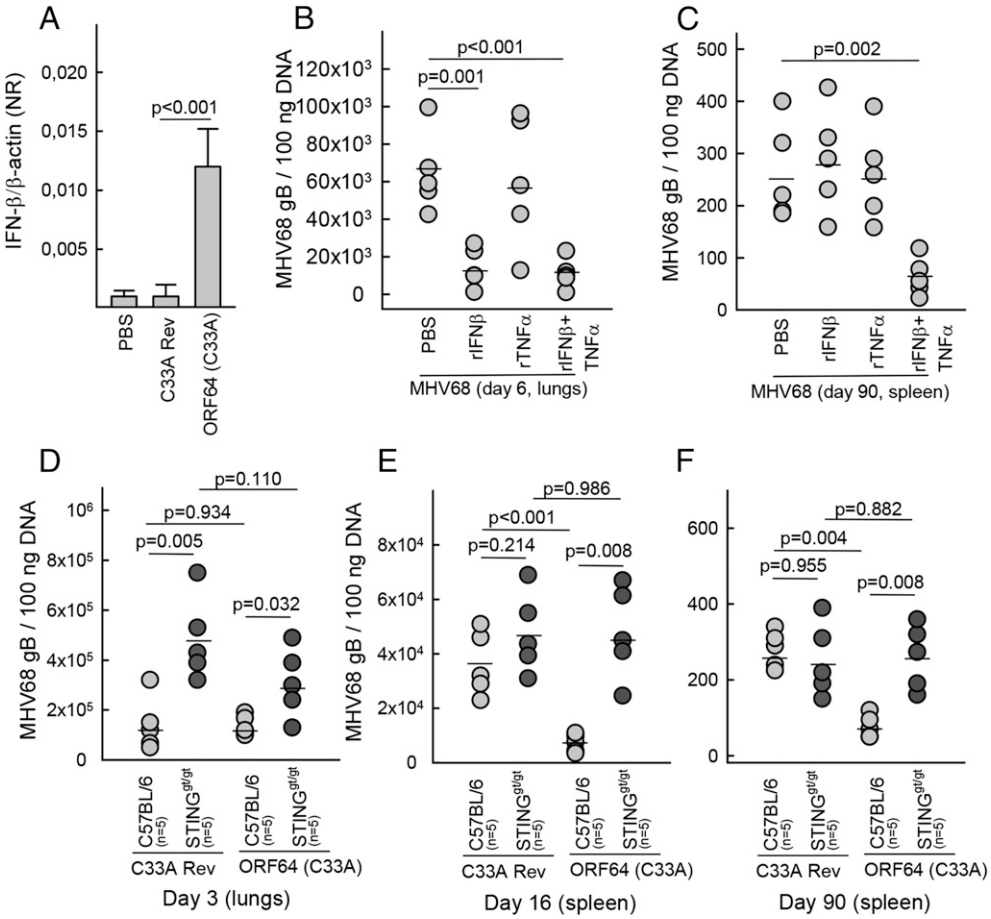

FIGURE 6. ORF64 DUB activity facilitates establishment of latency by targeting a STING-dependent pathway. (**A**) RNA was isolated from lung homogenates from C57BL/6 mice ($n = 5$ mice/group) 3 d after intranasal treatment with PBS, MHV68 ORF64 C33A, or the revertant virus (5×10^4 PFU). RNA was analyzed for levels of IFN-β mRNA by quantitative real-time PCR and presented as a normalized ratio (NR) using β-actin as internal reference. Data are mean ± SD. (**B** and **C**) C57BL/6 mice were treated i.p. with rIFN-β and rTNF-α (2 μg of each cytokine) at the time of intranasal MHV68 infection (5×10^4 PFU) and every 7 d during infection. Lungs were isolated from mice infected for 6 d (B), and spleens were isolated from mice infected for 90 d (C). Organs were homogenized and analyzed for the presence of MHV68 DNA by PCR. Each symbol represents an individual mouse. (**D**–**F**) C57BL/6 and $STING^{gt/gt}$ mice were infected intranasally with 5×10^4 PFU of MHV68 ORF64 C33A or the revertant virus. Lungs were isolated from mice infected for 3 d (D), and spleens were isolated from mice infected for 16 d (E) or 90 d (F). Organs were homogenized and analyzed for the presence of MHV68 DNA by PCR. Each symbol represents an individual mouse.

(38). Herpesviruses were reported to target all steps in the pathway, including modulation of PAMPs (39), avoidance of sensing (40), inhibition of signaling (41), and inhibition of transcription of key genes, including IFN-β (5, 42). In this study, we found that WT MHV68 largely prevented expression of type I IFN in macrophages and myeloid DCs, and it induced only modest levels of IL-1β. In contrast, it was shown that MHV68 induces type I IFN expression in plasmacytoid DCs and mouse embryonic fibroblasts, and this is stimulated through TLR-dependent pathways (19, 35). Altogether, such data suggest that MHV68 uses cell-type–specific means to evade innate immune responses and that ORF64 is of importance in cell types sensing this virus through the DNA-sensing pathway. Other reported innate immune-evasion mechanisms of MHV68 include targeting of TBK1 and IFN regulatory factor 3 by ORF11 and ORF36, respectively (22, 43). With regard to the known roles of herpesvirus tegument DUBs in innate immune evasion, most information has been gathered through work in HEK293 cell–based systems. It was reported that KSHV ORF64 can target RIG-I through deubiquitination of RIG-I (44) and that the EBV DUB BPLF1 inhibits the TLR2 pathway by deubiquitination of TRAF6, NEMO, and IκBα (45). Using a similar system, it also was demonstrated that HSV-1 UL36 can target TRAF3 to prevent type I IFN expression through the RIG-I pathway (46). However, in contrast to the studies mentioned above, which were performed primarily in overexpression systems (44–46), we found no inhibitory effects of MHV68 infection on induction of type I IFN and IL-6 by Sendai virus and TLR ligands. Moreover, the MHV68 DUB mutant induced elevated expression of both type I IFN and IL-1β compared with the WT virus, and the IFN response was evoked through the DNA-stimulated STING pathway. Therefore, our data do not support a model in which the MHV68 DUB targets a specific TRAF protein during viral infection in myeloid cells, rather, the virus targets a step at the level of DNA sensing upstream of bifurcation between the STING and AIM2 pathways. The herpesvirus DUB activity embedded in the N-terminal part of the large tegument protein is highly conserved (31). Because this activity can cleave either K48- or K63-linked polyubiquitin chains, it seems likely that herpesvirus DUBs can serve a broad role in targeting of intracellular innate-sensing and signaling pathways, as reported previously (44–46), and that this occurs in a manner dependent on a range of factors, including cell types and the stage of the viral replication cycle.

The establishment of latent gammaherpesvirus infections involves a complex series of events governed by viral proteins, with a particularly important role for the latency-associated nuclear Ag (47). In addition, several host systems are positively and nega-

tively involved in the establishment of latency, including IFNs, apoptosis, autophagy, and TLRs (47). We found that the DUB mutant virus, which activated STING-dependent innate immune responses, exhibited an impaired ability to establish latent infection in the spleen. The mechanism mediating this STING-dependent restriction of latency was not identified in this study, and further work is needed to describe the pathway capable of controlling DUB-deficient MHV68. Previous work revealed that the route of viral infection impacts on the apparent role for specific proteins in the host response to MHV68 infection (19). The same may be the case for the ability of MHV68 to facilitate establishment of latency through targeting of the DNA-sensing machinery. Published data on latent viral load in the spleen of C57BL/6 mice after i.p. infection with the MHV68 ΔDUB mutants did not reveal an attenuated phenotype of the virus (21).

Collectively, in this article we report that gammaherpesviruses evade sensing of viral genomic DNA, which facilitates establishment of a latent viral reservoir in the host. These data are consistent with a role for the gammaherpesvirus DUB in the prevention of innate immune activation by the viral DNA and suggest that the molecular target is upstream of bifurcation into the AIM2 and STING pathways. The STING-dependent antiviral program impaired by ORF64 works together with TLR-mediated activities to control acute and latent MHV68 infection. We propose that the ability of gammaherpesviruses to deubiquitinate viral and cellular substrates plays an important role in viral immune evasion and, hence, establishment of infection.

Acknowledgments

We thank Kirsten Stadel Petersen for technical assistance.

Disclosures

The authors have no financial conflicts of interest.

References

1. Pellet, P. E., and B. Roizman. 2007. The Family Herpesviridae: A brief introduction. In *Field's Virology*, 5th Ed. D. M. Knipe, P. M. Howley, D. E. Griffin, R. A. Lamb, M. A. Martin, B. Roizman, and S. E. Straus, eds. Lippincott-Williams and Wilkins, New York. p. 2479–2499.
2. Ishikawa, H., Z. Ma, and G. N. Barber. 2009. STING regulates intracellular DNA-mediated, type I interferon-dependent innate immunity. *Nature* 461: 788–792.
3. Reinert, L. S., L. Harder, C. K. Holm, M. B. Iversen, K. A. Horan, F. Dagnæs-Hansen, B. P. Ulhøi, T. H. Holm, T. H. Mogensen, T. Owens, et al. 2012. TLR3 deficiency renders astrocytes permissive to herpes simplex virus infection and facilitates establishment of CNS infection in mice. *J. Clin. Invest.* 122: 1368–1376.
4. Rathinam, V. A., Z. Jiang, S. N. Waggoner, S. Sharma, L. E. Cole, L. Waggoner, S. K. Vanaja, B. G. Monks, S. Ganesan, E. Latz, et al. 2010. The AIM2 inflammasome is essential for host defense against cytosolic bacteria and DNA viruses. *Nat. Immunol.* 11: 395–402.
5. Paludan, S. R., A. G. Bowie, K. A. Horan, and K. A. Fitzgerald. 2011. Recognition of herpesviruses by the innate immune system. *Nat. Rev. Immunol.* 11: 143–154.
6. Kawai, T., and S. Akira. 2011. Toll-like receptors and their crosstalk with other innate receptors in infection and immunity. *Immunity* 34: 637–650.
7. Tabeta, K., P. Georgel, E. Janssen, X. Du, K. Hoebe, K. Crozat, S. Mudd, L. Shamel, S. Sovath, J. Goode, et al. 2004. Toll-like receptors 9 and 3 as essential components of innate immune defense against mouse cytomegalovirus infection. *Proc. Natl. Acad. Sci. USA* 101: 3516–3521.
8. Lund, J., A. Sato, S. Akira, R. Medzhitov, and A. Iwasaki. 2003. Toll-like receptor 9-mediated recognition of Herpes simplex virus-2 by plasmacytoid dendritic cells. *J. Exp. Med.* 198: 513–520.
9. West, J. A., S. M. Gregory, V. Sivaraman, L. Su, and B. Damania. 2011. Activation of plasmacytoid dendritic cells by Kaposi's sarcoma-associated herpesvirus. *J. Virol.* 85: 895–904.
10. Unterholzner, L., S. E. Keating, M. Baran, K. A. Horan, S. B. Jensen, S. Sharma, C. M. Sirois, T. Jin, E. Latz, T. S. Xiao, et al. 2010. IFI16 is an innate immune sensor for intracellular DNA. *Nat. Immunol.* 11: 997–1004.
11. Zhang, Z., B. Yuan, M. Bao, N. Lu, T. Kim, and Y. J. Liu. 2011. The helicase DDX41 senses intracellular DNA mediated by the adaptor STING in dendritic cells. *Nat. Immunol.* 12: 959–965.
12. Takaoka, A., Z. Wang, M. K. Choi, H. Yanai, H. Negishi, T. Ban, Y. Lu, M. Miyagishi, T. Kodama, K. Honda, et al. 2007. DAI (DLM-1/ZBP1) is a cytosolic DNA sensor and an activator of innate immune response. *Nature* 448: 501–505.
13. Li, T., B. A. Diner, J. Chen, and I. M. Cristea. 2012. Acetylation modulates cellular distribution and DNA sensing ability of interferon-inducible protein IFI16. *Proc. Natl. Acad. Sci. USA* 109: 10558–10563.
14. Kerur, N., M. V. Veettil, N. Sharma-Walia, V. Bottero, S. Sadagopan, P. Otageri, and B. Chandran. 2011. IFI16 acts as a nuclear pathogen sensor to induce the inflammasome in response to Kaposi Sarcoma-associated herpesvirus infection. *Cell Host Microbe* 9: 363–375.
15. Sun, L., J. Wu, F. Du, X. Chen, and Z. J. Chen. 2013. Cyclic GMP-AMP synthase is a cytosolic DNA sensor that activates the type I interferon pathway. *Science* 339: 786–791.
16. Hornung, V., A. Ablasser, M. Charrel-Dennis, F. Bauernfeind, G. Horvath, D. R. Caffrey, E. Latz, and K. A. Fitzgerald. 2009. AIM2 recognizes cytosolic dsDNA and forms a caspase-1-activating inflammasome with ASC. *Nature* 458: 514–518.
17. Horan, K. A., K. Hansen, M. R. Jakobsen, C. K. Holm, S. Søby, L. Unterholzner, M. Thompson, J. A. West, M. B. Iversen, S. B. Rasmussen, et al. 2013. Proteasomal degradation of herpes simplex virus capsids in macrophages releases DNA to the cytosol for recognition by DNA sensors. *J. Immunol.* 190: 2311–2319.
18. Fiola, S., D. Gosselin, K. Takada, and J. Gosselin. 2010. TLR9 contributes to the recognition of EBV by primary monocytes and plasmacytoid dendritic cells. *J. Immunol.* 185: 3620–3631.
19. Guggemoos, S., D. Hangel, S. Hamm, A. Heit, S. Bauer, and H. Adler. 2008. TLR9 contributes to antiviral immunity during gammaherpesvirus infection. *J. Immunol.* 180: 438–443.
20. Adler, H., M. Messerle, M. Wagner, and U. H. Koszinowski. 2000. Cloning and mutagenesis of the murine gammaherpesvirus 68 genome as an infectious bacterial artificial chromosome. *J. Virol.* 74: 6964–6974.
21. Gredmark-Russ, S., M. K. Isaacson, L. Kattenhorn, E. J. Cheung, N. Watson, and H. L. Ploegh. 2009. A gammaherpesvirus ubiquitin-specific protease is involved in the establishment of murine gammaherpesvirus 68 infection. *J. Virol.* 83: 10644–10652.
22. Hwang, S., K. S. Kim, E. Flano, T. T. Wu, L. M. Tong, A. N. Park, M. J. Song, D. J. Sanchez, R. M. O'Connell, G. Cheng, and R. Sun. 2009. Conserved herpesviral kinase promotes viral persistence by inhibiting the IRF-3-mediated type I interferon response. *Cell Host Microbe* 5: 166–178.
23. Bolstad, M., F. Abaitua, C. M. Crump, and P. O'Hare. 2011. Autocatalytic activity of the ubiquitin-specific protease domain of herpes simplex virus 1 VP1-2. *J. Virol.* 85: 8738–8751.
24. Upton, J. W., W. J. Kaiser, and E. S. Mocarski. 2010. Virus inhibition of RIP3-dependent necrosis. *Cell Host Microbe* 7: 302–313.
25. Redwood, A. J., M. Messerle, N. L. Harvey, C. M. Hardy, U. H. Koszinowski, M. A. Lawson, and G. R. Shellam. 2005. Use of a murine cytomegalovirus K181-derived bacterial artificial chromosome as a vaccine vector for immunocontraception. *J. Virol.* 79: 2998–3008.
26. Choi, M. K., Z. Wang, T. Ban, H. Yanai, Y. Lu, R. Koshiba, Y. Nakaima, S. Hangai, D. Savitsky, M. Nakasato, et al. 2009. A selective contribution of the RIG-I-like receptor pathway to type I interferon responses activated by cytosolic DNA. *Proc. Natl. Acad. Sci. USA* 106: 17870–17875.
27. Jakobsen, M. R., R. O. Bak, A. Andersen, R. K. Berg, S. B. Jensen, J. Tengchuan, A. Laustsen, K. Hansen, L. Ostergaard, K. A. Fitzgerald, et al. 2013. IFI16 senses DNA forms of the lentiviral replication cycle and controls HIV-1 replication. *Proc. Natl. Acad. Sci. USA* 110: E4571–E4580.
28. Holm, C. K., S. B. Jensen, M. R. Jakobsen, N. Cheshenko, K. A. Horan, H. B. Moeller, R. Gonzalez-Dosal, S. B. Rasmussen, M. H. Christensen, T. O. Yarovinsky, et al. 2012. Virus-cell fusion as a trigger of innate immunity dependent on the adaptor STING. *Nat. Immunol.* 13: 737–743.
29. Usherwood, E. J., J. P. Stewart, K. Robertson, D. J. Allen, and A. A. Nash. 1996. Absence of splenic latency in murine gammaherpesvirus 68-infected B cell-deficient mice. *J. Gen. Virol.* 77: 2819–2825.
30. Wen, K. W., and B. Damania. 2010. Kaposi sarcoma-associated herpesvirus (KSHV): molecular biology and oncogenesis. *Cancer Lett.* 289: 140–150.
31. Kattenhorn, L. M., G. A. Korbel, B. M. Kessler, E. Spooner, and H. L. Ploegh. 2005. A deubiquitinating enzyme encoded by HSV-1 belongs to a family of cysteine proteases that is conserved across the family Herpesviridae. *Mol. Cell* 19: 547–557.
32. González, C. M., L. Wang, and B. Damania. 2009. Kaposi's sarcoma-associated herpesvirus encodes a viral deubiquitinase. *J. Virol.* 83: 10224–10233.
33. Wang, I. H., M. Suomalainen, V. Andriasyan, S. Kilcher, J. Mercer, A. Neef, N. W. Luedtke, and U. F. Greber. 2013. Tracking viral genomes in host cells at single-molecule resolution. *Cell Host Microbe* 14: 468–480.
34. Paludan, S. R., and A. G. Bowie. 2013. Immune sensing of DNA. *Immunity* 38: 870–880.
35. Michaud, F., F. Coulombe, E. Gaudreault, J. Kriz, and J. Gosselin. 2010. Involvement of TLR2 in recognition of acute gammaherpesvirus-68 infection. *PLoS ONE* 5: e13742.
36. Schoggins, J. W., D. A. Macduff, N. Imanaka, M. D. Gainey, B. Shrestha, J. L. Eitson, K. B. Mar, R. B. Richardson, A. V. Ratushny, V. Litvak, et al. 2014. Pan-viral specificity of IFN-induced genes reveals new roles for cGAS in innate immunity. *Nature* 505: 691–695.
37. Ansari, M. A., V. V. Singh, S. Dutta, M. V. Veettil, D. Dutta, L. Chikoti, J. Lu, D. Everly, and B. Chandran. 2013. Constitutive interferon-inducible protein 16-inflammasome activation during Epstein-Barr virus latency I, II, and III in B and epithelial cells. *J. Virol.* 87: 8606–8623.
38. Bowie, A. G., and L. Unterholzner. 2008. Viral evasion and subversion of pattern-recognition receptor signalling. *Nat. Rev. Immunol.* 8: 911–922.

39. Pezda, A. C., A. Penn, G. M. Barton, and L. Coscoy. 2011. Suppression of TLR9 immunostimulatory motifs in the genome of a gammaherpesvirus. *J. Immunol.* 187: 887–896.
40. Orzalli, M. H., N. A. DeLuca, and D. M. Knipe. 2012. Nuclear IFI16 induction of IRF-3 signaling during herpesviral infection and degradation of IFI16 by the viral ICP0 protein. *Proc. Natl. Acad. Sci. USA* 109: E3008–E3017.
41. Verpooten, D., Y. Ma, S. Hou, Z. Yan, and B. He. 2009. Control of TANK-binding kinase 1-mediated signaling by the gamma(1)34.5 protein of herpes simplex virus 1. *J. Biol. Chem.* 284: 1097–1105.
42. Zhu, F. X., S. M. King, E. J. Smith, D. E. Levy, and Y. Yuan. 2002. A Kaposi's sarcoma-associated herpesviral protein inhibits virus-mediated induction of type I interferon by blocking IRF-7 phosphorylation and nuclear accumulation. *Proc. Natl. Acad. Sci. USA* 99: 5573–5578.
43. Kang, H. R., W. C. Cheong, J. E. Park, S. Ryu, H. J. Cho, H. Youn, J. H. Ahn, and M. J. Song. 2014. Murine gammaherpesvirus 68 encoding open reading frame 11 targets TANK binding kinase 1 to negatively regulate the host type I interferon response. *J. Virol.* 88: 6832–6846.
44. Inn, K. S., S. H. Lee, J. Y. Rathbun, L. Y. Wong, Z. Toth, K. Machida, J. H. Ou, and J. U. Jung. 2011. Inhibition of RIG-I-mediated signaling by Kaposi's sarcoma-associated herpesvirus-encoded deubiquitinase ORF64. *J. Virol.* 85: 10899–10904.
45. van Gent, M., S. G. E. Braem, A. de Jong, N. Delagic, J. G. C. Peeters, I. G. J. Boer, P. N. Moynagh E. Kremmer, E. J. Wiertz, H. Ovaa, et al. 2014. Epstein-Barr virus large tegument protein BPLF1 contributes to innate immune evasion through interference with toll-like receptor signaling. *PLoS Pathog.* 10: e1003960.
46. Wang, S., K. Wang, J. Li, and C. Zheng. 2013. Herpes simplex virus 1 ubiquitin-specific protease UL36 inhibits beta interferon production by deubiquitinating TRAF3. *J. Virol.* 87: 11851–11860.
47. Barton, E., P. Mandal, and S. H. Speck. 2011. Pathogenesis and host control of gammaherpesviruses: lessons from the mouse. *Annu. Rev. Immunol.* 29: 351–397.